of tetraoxyphosphoranes rather than the use of P–O ring-bound oxygen atoms as studied previously.[12] In either case, chain and dimer formations resulted for the pentacoordinated spirocyclic phosphorus compounds with the rings situated axial–equatorially in trigonal-bipyramidal geometries. In contrast to the previous study[12] where hydrogen bonding gave boat and chair conformations for the six-membered ring, the present study gave chair conformations exclusively. Activation energies for intramolecular exchange interpreted in terms of a pseudorotational process requiring diequatorial placement of the phosphorinane ring in a TBP exchange intermediate were similar for the two classes of hydrogen-bonded compounds and suggested that the energy required for diequatorial placement of a phosphorinane ring (≥11 kcal/mol) in the ground state exceeds the available hydrogen-bond energy. Thus far, no evidence from solid-state studies has been obtained supporting a diequatorial orientation for a six-membered ring in an oxyphosphorane. These results suggest that if protein kinases in their interaction with *c*-AMP are capable of providing the energy necessary for the formation of phosphorane activated states proposed to contain (e-e) orientations,[13,15,16] a combination of active-site constraints may be required.

Acknowledgment. The support of this research by the National Science Foundation (Grant CHE88-19152) and the Army Research Office is gratefully acknowledged as is a helpful discussion with Professor W. E. McEwen.

Registry No. **1**, 135929-32-7; **2**, 135929-33-8; **3**, 24418-67-5; **4**, 135929-34-9; **5**, 74390-22-0; 2-amino-5-nitrophenol, 121-88-0; 2-amino-3-hydroxypyridine, 16867-03-1; 2-hydroxybenzyl alcohol, 90-01-7; 2-amino-4,6-dimethylphenol, 41458-65-5.

Supplementary Material Available: Tables of atomic coordinates, thermal parameters, additional bond lengths and angles, and hydrogen atom parameters (Tables S1–S4 for **1**, Tables S5–S8 for **2**, and Tables S9–S12 for **3**) (25 pages); listings of structure factors (25 pages). Ordering information is given on any current masthead page.

Contribution from the Department of Chemistry of the University of Florence, Florence, Italy, and Departement de Recherche Fondamentale, Centre d'Etudes Nucleaires de Grenoble, Grenoble, France

Structure and Magnetic Ordering of a Ferrimagnetic Helix Formed by Manganese(II) and a Nitronyl Nitroxide Radical

Andrea Caneschi,[†] Dante Gatteschi,*[,†] Paul Rey,[‡] and Roberta Sessoli[†]

Received February 13, 1991

A chain compound of formula $Mn(hfac)_2NITPhOMe$, where hfac = hexafluoroacetylacetonato and NITPhOMe = 2-(4-methoxyphenyl)-4,4,5,5-tetramethylimidazoline-1-oxyl 3-oxide, was synthesized, and the X-ray analysis showed that it crystallizes in the trigonal acentric $P3_1$ space group with a = 11.131 (3) Å, c = 20.846 (9) Å, and Z = 3. The structure consists of helices in which the $Mn(hfac)_2$ moieties are bridged by the radicals coordinated through the two equivalent oxygen atoms. The magnetic susceptibility in the form χT vs T shows a marked increase on lowering the temperature, and a numerical fitting indicated a strong antiferromagnetic intrachain interaction (J = 344 cm^{-1}). The uncompensation of the $S = {}^5/_2$ spin of manganese(II) and $S = {}^1/_2$ spin of the radical originates high resultant magnetic moments, and at ca. 4.8 K the system orders three-dimensionally as confirmed by AC susceptibility measurements in nearly zero field. Magnetization measurements indicate that the system orders ferrimagnetically with S = 2, as expected for antiparallel alignment of $S = {}^5/_2$ and $S = {}^1/_2$. Single-crystal EPR spectra at variable temperatures revealed a pure xy anisotropy with the easy plane perpendicular to the helix axis c. The calculation of the dipolar anisotropy performed within the point dipole approximation reproduces the observed behavior. The transition temperature and the dipolar energies are compared with those of two other $Mn(hfac)_2NITR$ chains, and magneto–structural correlations that justify the experimental trend in critical temperature are presented. The acentric space group allows nonlinear optical activity, and preliminary measurements show a sizeable SHG activity at 1064 nm, which must essentially be associated with the radical.

Introduction

Molecular based magnetic materials are compounds exhibiting spontaneous magnetization below a critical temperature, T_c, that are formed by molecular entities, even if they do not necessarily correspond to molecular lattices. Beyond the challenge of designing and synthesizing new classes of compounds it is hoped that the properties of these materials can be finely tuned by exploiting the techniques of molecular chemistry.[1-7] Since the magnetic properties are determined by the spatial arrangement of the interacting magnetic centers, it is necessary to learn the most appropriate ways of assembling them in a lattice in order to maximize the interactions.

A potentially interesting feature of these materials is that in principle they might show an unusual association of properties, for instance magnetic and optical, magnetic and electrical, and magnetic and chemical, that are bound to their molecular nature.[8] This is a field that has not yet been fully exploited and deserves much attention. In particular, since among the possible uses that can be envisaged for molecular based magnetic materials exhibiting spontaneous magnetization, magneto–optical effects are of paramount interest, it is very important to design materials that can show unusual optical properties associated with spontaneous magnetization.

We are currently studying materials that are formed by the interaction of metal ions and nitronyl nitroxides of formula 2-R-4,4,5,5-tetramethylimidazoline-1-oxyl 3-oxide, NITR.[7] In this

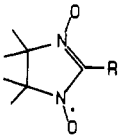

NITR

approach to molecular based magnetic materials the versatility is given by the possibility to change the metal ion and the R group

[†] University of Florence.
[‡] Centre d'Etudes Nucleaires de Grenoble.

(1) Miller, J. S.; Epstein, A. J.; Reiff, W. M. *Chem. Rev.* **1988**, *88*, 201. Miller, J. S.; Epstein, A. J.; Reiff, W. M. *Acc. Chem. Res.* **1988**, *21*, 114.
(2) Kahn, O. *NATO ASI Ser. B* **1987**, *168*, 93. Nakatani, K.; Carriat, J. Y.; Journaux, Y.; Kahn, O.; Lloret, F.; Renard, J. P.; Pei, Y.; Sletten, J.; Verdaguer, M. *J. Am. Chem. Soc.* **1989**, *111*, 5739.
(3) Korshak, Y. V.; Medvedeva, T. V.; Ovchinnikov, A. A.; Spector, V. N. *Nature* **1987**, *326*, 370.
(4) Iwamura, H. *Pure Appl. Chem.* **1986**, *58*, 187.
(5) Le Page, T. J.; Breslow, R. *J. Am. Chem. Soc.* **1987**, *109*, 6412.
(6) Torrance, J. B.; Oostra, S.; Nazzal, A. *Synth. Met.* **1987**, *19*, 708.
(7) Caneschi, A.; Gatteschi, D.; Sessoli, R.; Rey, P. *Acc. Chem. Res.* **1989**, *22*, 329.
(8) Miller, J. S. *Adv. Mater.* **1990**, *2*, 98.

0020-1669/91/1330-3936$02.50/0

Table I. Crystal Data and Experimental Parameters for $Mn(hfac)_2NITPhOMe$

formula	$MnC_{24}H_{21}N_2O_7F_{12}$	Z	3
fw	732.36	D(calcd)	1.631 g/cm^3
cryst system	trigonal	μ(Mo Kα)	5.40 cm^{-1}
space group	$P3_1$	temp	298 K
a	11.131 (3) Å	radiation (λ)	Mo Kα (0.710 73 Å)
c	20.846 (9) Å		
V	2237 Å^3	refinement	R = 0.070, R_w = 0.078

of the radical and to induce changes in the coordination geometries. The most interesting results were obtained so far with $Mn(hfac)_2NITR$ compounds (hfac = hexafluoroacetylacetonato; R = ethyl, isopropyl, *n*-propyl), which behave as one-dimensional ferrimagnets at high temperatures and order ferromagnetically at low temperature. In fact T_c ranges from 7.6 to 8.5 K depending on R.[9,11] Our understanding of the mechanism responsible for the three-dimensional order in these materials is that the strong antiferromagnetic coupling occurring between manganese and radicals in the chains determines a strong correlation of the spins in such a way that even the weak dipolar interaction between the chains is sufficient to cause magnetic order at low temperatures.

The factors that can be expected to influence the transition temperature are the distance between the chains, a larger distance determining a lower T_c; the exchange interaction within the chain, a stronger interaction determining a higher T_c; and also the magneto-crystalline anisotropy, which is of fundamental importance in the determination of T_c. In fact it is well-known that the transition temperature from 1-D to 3-D behavior increases on going from xy to Ising anisotropy.[12] Ideally one should be able to optimize all these parameters in order to increase T_c for metal–nitronyl nitroxides compounds.

With these considerations in mind, we have synthesized a compound of formula $Mn(hfac)_2NITPhOMe$, where R = 4-methoxyphenyl, which has a unique helix structure, which is very appealing to investigate complex structure–property correlations. In particular we want to show how the structural features of $Mn(hfac)_2NITPhOMe$ differentiate it from other analogous compounds and how magneto-crystalline anisotropy is of paramount importance in determining the critical temperature of $Mn(hfac)_2NITR$ chains. Further, $Mn(hfac)_2NITPhOMe$ is the first compound reported that associates bulk ferromagnetism with nonlinear optical, NLO, properties.

Experimental Section

Synthesis of the Complex. $Mn(hfac)_2{\cdot}2H_2O$ was prepared as previously described.[13] The NITPhOMe radical was prepared according to the method reported in literature for the phenyl derivative, NITPh,[14] by using 4-methoxybenzaldehyde rather than benzaldehyde to condensate the 2,3-bis(hydroxylamino)-2,3-dimethylbutane precursor.

$Mn(hfac)_2{\cdot}2H_2O$ (0.5 mmol) was dissolved in hot *n*-heptane, and then 0.5 mmol of NITPhOMe radical was added. The solution was allowed to cool down to room temperature and then stored at 4 °C for 1 week. Elongated dark green crystals, suitable for X-ray analysis, were collected and analyzed well for $Mn(hfac)_2NITPhOMe$. Anal. Calcd for $C_{24}F_{12}H_{21}MnN_2O_7$: C, 39.36; H, 2.89; N, 3.83. Found: C, 39.29; H, 2.97; N, 3.67.

X-ray Structure Determination. The intensity data were collected at room temperature on a CAD4 Enraf-Nonius four-circle diffractometer. Details on crystal and experimental parameters are reported in Table SI (supplementary material) and in Table I in a condensed form. The compound crystallizes in the hexagonal system, and systematic absences together with density considerations indicated the two enantiomeric space groups $P3_1$ and $P3_2$. The metal coordinates were found by a Patterson map, while the other non-hydrogen atoms were revealed by successive Fourier synthesis using the SHELX76 package.[15] The full-matrix least-squares refinement and an empirical correction for absorption[16] were performed for the two space groups. The final refinement including the contribution of hydrogen atoms in idealized positions gave R = 7.0 and R_w = 7.8 for $P3_1$ space group and R = 7.6 and R_w = 8.2 for the $P3_2$ one. The first space group was considered correct with a significance level better than 0.99.[17]

The structure solution was characterized by a large and anisotropic thermal motion and/or disorder of the CF_3 groups and of the carbon atom of the methoxy group. However, it did not affect seriously the precision of the structure around the metal center and peaks less than 0.5 e/Å^3 were found in the last Fourier difference map. Final coordinates and isotropic thermal factors are reported in Table II.

Physical Measurements. The magnetic susceptibility of a powder sample in the temperature range 2–300 K at a field strength of 100 Oe and magnetization in variable fields were measured by an SHE SQUID magnetometer.

Low-field measurements were performed on a laboratory-assembled AC susceptometer based on a mutual inductance bridge[18] measuring both

Table II. Positional Parameter (×10^4) and Isotropic Thermal Factors (×10^3) for $Mn(hfac)_2NITPhOMe$[a]

	x/a	y/b	z/c	U_{iso}, Å^2
Mn	8808 (1)	3991 (1)	0	52
O1	8250 (6)	5355 (6)	−424 (3)	72
O2	10052 (6)	5670 (6)	623 (3)	66
O3	10486 (6)	4943 (6)	−697 (3)	69
O4	9796 (6)	2862 (6)	195 (3)	73
O5	7383 (5)	3238 (6)	781 (2)	62
O6	7343 (5)	2275 (5)	−530 (2)	59
O7	7087 (10)	8824 (8)	737 (4)	128
N1	7562 (5)	3435 (5)	1383 (3)	48
N2	7730 (6)	4304 (6)	2335 (3)	56
C1	8991 (9)	6636 (9)	−407 (4)	75
C2	10479 (9)	6904 (9)	491 (4)	73
C3	10001 (10)	7401 (10)	9 (4)	79
C4	8612 (14)	7349 (12)	−952 (6)	110
C5	11608 (11)	7928 (11)	916 (6)	100
C6	11537 (9)	4913 (9)	−694 (4)	75
C7	10859 (10)	3053 (11)	53 (5)	89
C8	11815 (12)	4017 (12)	−368 (5)	98
C9	12682 (11)	5967 (13)	−1123 (6)	115
C10	11307 (15)	2053 (18)	376 (9)	157
C11	7540 (7)	4462 (8)	1707 (3)	49
C12	7574 (9)	2413 (10)	1816 (4)	78
C13	8119 (11)	3258 (10)	2437 (4)	81
C14	8457 (16)	1864 (13)	1542 (5)	128
C15	6049 (15)	1285 (10)	1885 (5)	134
C16	9660 (15)	4029 (15)	2447 (6)	128
C17	7594 (19)	2530 (14)	3057 (4)	146
C18	7356 (7)	5548 (7)	1450 (3)	54
C19	8127 (8)	6845 (8)	1692 (4)	62
C20	8074 (10)	7965 (10)	1429 (4)	82
C21	7141 (10)	7700 (10)	958 (5)	81
C22	6316 (10)	6408 (10)	713 (5)	82
C23	6411 (9)	5297 (9)	961 (4)	65
C24	6125 (18)	8617 (17)	233 (7)	154
F1	7339 (10)	7058 (11)	−876 (5)	168
F2	8576 (11)	6809 (12)	−1506 (4)	180
F3	9349 (15)	8602 (10)	−960 (7)	264
F4	11457 (8)	7559 (8)	1521 (3)	143
F5	12751 (7)	7977 (12)	752 (5)	187
F6	11816 (11)	9149 (7)	900 (5)	195
F7	12269 (11)	6440 (12)	−1565 (6)	219
F8	13255 (14)	5500 (13)	−1460 (7)	245
F9	13553 (16)	6886 (15)	−837 (6)	321
F10	11484 (14)	1307 (12)	−142 (7)	211
F11	10519 (13)	1242 (16)	723 (8)	310
F12	12652 (12)	2762 (14)	540 (5)	199

[a] Standard deviations in the last significant digit are given in parentheses.

(9) Caneschi, A.; Gatteschi, D.; Rey, P.; Sessoli, R. *Inorg. Chem.* **1988**, *27*, 1756.
(10) Caneschi, A.; Gatteschi, D.; Renard, J. P.; Rey, P.; Sessoli, R. *Inorg. Chem.* **1989**, *28*, 1976.
(11) Caneschi, A.; Gatteschi, D.; Renard, J. P.; Rey, P.; Sessoli, R. *Inorg. Chem.* **1989**, *28*, 3314.
(12) Renard, J. P. *NATO ASI Ser. B* **1987**, *168*, 125.
(13) Cotton, F. A.; Holm, R. H. *J. Am. Chem. Soc.* **1960**, *86*, 2979.
(14) Ullman, E. F.; Osiecky, J. H.; Boocock, D. C. B.; Darcy, R. *J. Am. Chem. Soc.* **1972**, *94*, 7049.
(15) Sheldrick, G. SHELX76 System of Computing Programs. University of Cambridge, Cambridge, England, 1976. Atomic scattering factors are after: Cromer, D. T.; Lieberman, D. *J. Chem. Phys.* **1970**, *53*, 1891.
(16) Walker, N.; Stuart, D. *Acta Crystallogr.* **1983**, *A38*, 158.
(17) Hamilton, W. C. *Acta Crystallogr.* **1965**, *18*, 502.

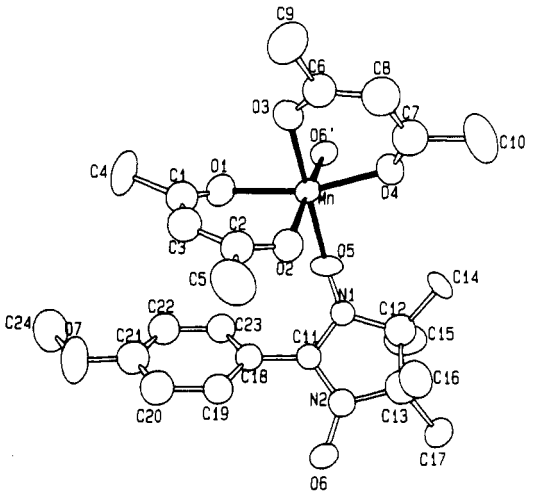

Figure 1. ORTEP view at 50% probability of the asymmetric unit of $Mn(hfac)_2NITPhOMe$. The fluorine atoms were omitted for clarity.

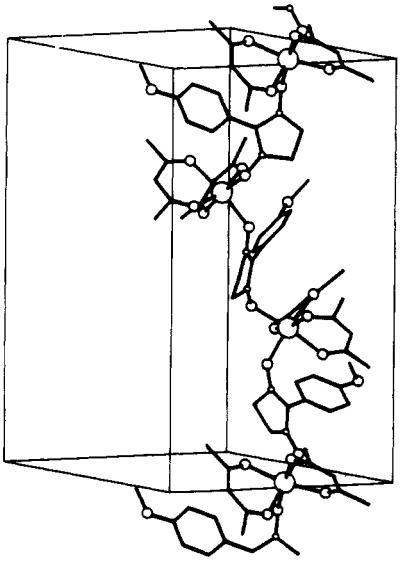

Figure 2. Simplified view of the content of the unit cell of $Mn(hfac)_2NITPhOMe$. The chain develops along the unique axis *c*.

the real and imaginary component of the magnetic susceptibility. The sample was introduced in a fused silica Dewar vessel immersed in liquid helium of a liquid-nitrogen-shielded cryostat. A low pressure of helium gas kept a weak thermal contact with the cryogenic bath. The temperature was measured with a calibrated gallium–aluminum arsenide diode placed on the sample.

The measurements were performed at a frequency of 333 Hz in zero static field with an alternating field of 0.8 Oe.

EPR spectra were recorded with a Varian E9 spectrometer at X-band frequency. Variable-temperature spectra in the range 4.2–300 K were recorded by using an Oxford Instruments ESR9 liquid-helium continuous-flow cryostat.

A single crystal was oriented with the diffractometer mentioned above and was found to have the shape of a hexagonal rod elongated along *c* and with the faces (±100) largely developed. It was mounted on a sample holder that permitted rotation along the $a^* = b \times c$ axis.

Results and Discussion

Crystal Structure. The structure consists of manganese(II) ions octahedrally coordinated by the oxygen atoms of the hfac molecules and those of two nitronyl nitroxides that are cis to each other. The asymmetric unit is sketched in Figure 1. O6 is bound to an adjacent manganese atom thus bridging the metal units to give a chain that develops along the crystallographic axis *c*, as shown in Figure 2. This metal–radical arrangement is known to be particularly well suited to yield extended magnetic interactions.[7,9,19,20] However, the present compound has the unique feature that the chains are developed as helices, as demanded by the crystallographic 3_1 symmetry. The noncentric space group was confirmed by the observation of optical second harmonic generation, SHG. Powder tests[21] carried out by using a Q-switched Nd–YAG laser emitting at $\lambda = 1064$ nm showed that radiation at $\lambda = 532$ nm is generated. The UV–vis spectrum of $Mn(hfac)_2NITPhOMe$ in KBr pellets is very similar to that of a solution of a pure radical, and the strongest absorptions can be safely attributed to $n \rightarrow \pi^*$, a very broad band centered around 680 nm, to $\pi \rightarrow \pi^*$ of the ONCNO coniugate group of the radical, 370 nm, and to $\pi \rightarrow \pi^*$ of the benzene ring, 280 nm. The generated frequency is thus partially absorbed, and the compound decomposes due to the high power necessary in this preliminary experimental setup. Therefore, it is not possible to provide a quantitative assessment of the second-order susceptibility, χ^2. Similar SHG properties and strong absorption were recently reported for the free radical $NITpNO_2Ph$,[22] suggesting that the large polarizability required for NLO is associated with the radical. The metal ions in this case provide a suitable acentric framework to keep the radicals properly oriented in the lattice.

Table III. Selected Bond Distances (Å) and Angles (deg) for $Mn(hfac)_2NITPhOMe$[a]

Mn–O1	2.129 (8)	Mn–O2	2.145 (5)
Mn–O3	2.197 (6)	Mn–O4	2.089 (8)
Mn–O5	2.145 (5)	Mn–O6	2.125 (5)
O5–N1	1.273 (7)	O6–N2	1.296 (9)
N1–C11	1.354 (11)	N2–C11	1.353 (10)
O5–Mn–O6	86.8 (2)	O4–Mn–O6	87.1 (2)
O4–Mn–O5	97.3 (2)	O3–Mn–O6	101.1 (2)
O3–Mn–O5	171.8 (2)	O3–Mn–O4	81.0 (3)
O2–Mn–O6	171.9 (2)	O2–Mn–O5	85.5 (2)
O2–Mn–O4	96.4 (3)	O2–Mn–O3	86.7 (2)
O1–Mn–O6	93.9 (2)	O1–Mn–O5	99.6 (2)
O1–Mn–O4	163.2 (3)	O1–Mn–O3	82.4 (2)
O1–Mn–O2	84.8 (2)	Mn–O5–N1	131.0 (5)
Mn–O6–N2	127.7 (4)	O6–N2–C11	126.3 (7)
O5–N1–C11	124.9 (6)		

[a] Standard deviations in the last significant digit are given in parentheses.

The octahedron around the manganese is rather distorted with Mn–O distances ranging from 2.089 (8) to 2.197 (6) Å. Selected bond lengths and angles are reported in Table III. In order to accommodate the two nitronyl nitroxides in cis positions, the two hfac molecules deviate significantly from octahedral coordination, and in particular, the O1–Mn–O4 angle is 163.2 (3)°. The two NO distances are rather different from each other, being 1.273 (7) vs 1.296 (9) Å, but the rest of the radical is fairly normal.[19] The average plane of the unsaturated part of the radical, ONCNO, forms an angle of 42.3° with that of the phenyl ring.

An interesting structural feature of the present compound is the stacking interaction between the phenyl ring and the unsaturated part of two hfac molecules of the two adjacent metal centers. The average planes form an angle of about 11°, and the shortest contacts are O3–C18 = 3.56 Å and O1–C18 = 4.26 Å for the two hfac molecules, respectively. This kind of stacking has already been observed in the hexanuclear compound $[Mn(hfac)_2NITPh]_6$ in which this interaction has been suggested as the driving force toward the formation of the ring structure.[23] In both compounds the space group is hexagonal, a necessary feature to have the hfac and the phenyl ring of adjacent units in close contact. The hexagonal symmetry is retained in that each chain

(18) The susceptibility probe was designed and built by B. Lecuyer of the "Institut d'Electronique Fondamentale", Universite Paris-Sud, Orsay, France.

(19) Caneschi, A.; Gatteschi, D.; Rey, P. *Prog. Inorg. Chem.*, in press.
(20) Cabello, C. I.; Caneschi, A.; Gatteschi, D.; Rey, P.; Sessoli, R. *Inorg. Chem.* **1990**, *29*, 2582.
(21) Kurtz, S. K.; Perry, T. T. *J. Appl. Phys.* **1968**, *39*, 3798.
(22) Wudl, F. *Abstracts of Papers*, 199th National Meeting of the American Chemical Society, in press.
(23) Caneschi, A.; Gatteschi, D.; Laugier, J.; Rey, P.; Sessoli, R.; Zanchini, C. *J. Am. Chem. Soc.* **1988**, *110*, 2307.

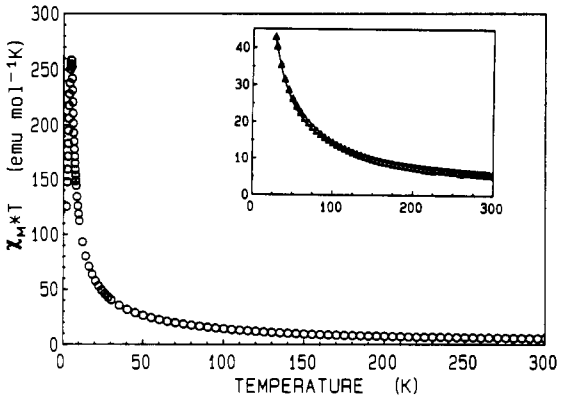

Figure 3. Temperature dependence of the product of the magnetic susceptibility with temperature for $Mn(hfac)_2NITPhOMe$. In the inset are reported the calculated values with the best fit parameter J = 344 cm^{-1}.

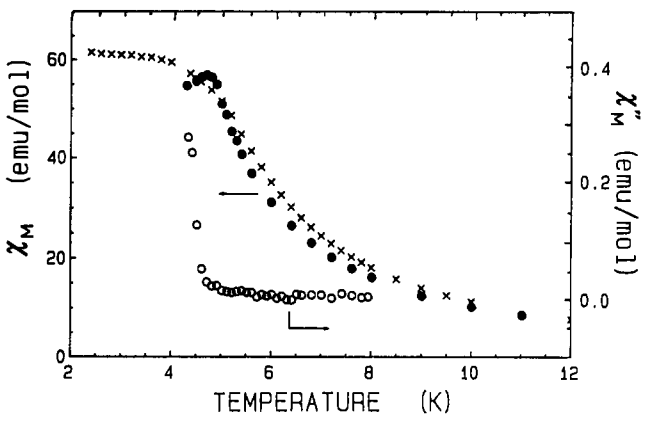

Figure 4. Magnetic susceptibility for $Mn(hfac)_2NITPhOMe$: (×) susceptibility measured in 100-Oe external field; (●) real part of the AC susceptibility measured at 333 Hz and zero static field; (○) imaginary part of the AC susceptibility.

is surrounded by six equivalent chains at 11.131 (3) Å, the distance estimated as the shortest Mn–Mn contact.

Magnetic Properties. The temperature dependence of the magnetic susceptibility is reported in Figure 3. The room-temperature value χT = 5.5 emu K mol^{-1} (μ_{eff} = 6.6 μ_B), is higher than the value expected for uncorrelated $S = {}^5/_2$ and $S = {}^1/_2$ spins (4.75 emu K mol^{-1}). On decrease of the temperature, an increase in the χT value is observed, which accelerates below 50 K. This behavior has already been observed in other alternating spin chains[9-11,24-27] and is due to the fact that the interaction is not limited to a finite number of spins but at low temperature a large number of individual magnetic moments are correlated. Since the manganese and radical spins are different in magnitude, even their antiparallel alignment yields a large effective magnetic moment and consequently a large value of χT.

The experimental susceptibility has been reproduced by using the nearest-neighbor Heisenberg model that treats the spin ${}^1/_2$ of the radical as quantized and the spin ${}^5/_2$ of manganese(II) as classic.[28] The best fit was obtained with an antiferromagnetic coupling constant of 344 (1) cm^{-1}, the Hamiltonian being defined as $H = J\sum S_i S_{i-1}$. The g factor of both spins was fixed at 2.0.[29] This value of the coupling constant is the highest yet reported for a chain compound containing manganese(II) and nitronyl nitroxides. In particular it is much higher than that observed for the

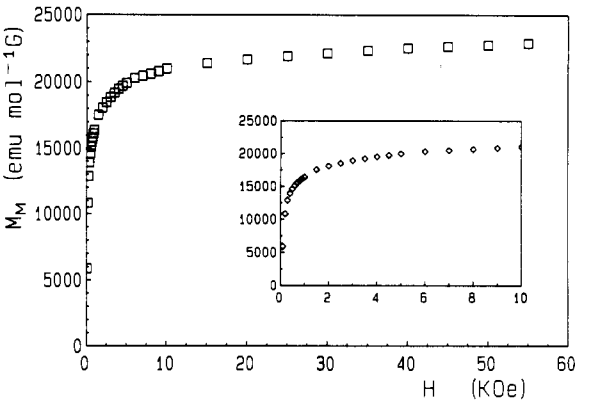

Figure 5. Magnetization vs magnetic field for $Mn(hfac)_2HITPhOMe$. In the inset the low-field region is reported in an expanded scale.

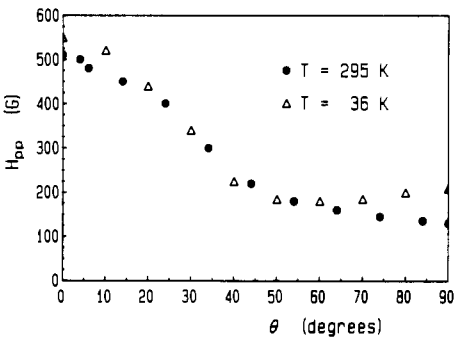

Figure 6. Angular dependence of the line width of the EPR spectra at two temperatures and 9.25 GHz. θ is the angle of the magnetic field with the c axis.

phenyl derivative (208 cm^{-1}).[9] The inductive effect of the methoxy group, which enhances the electron density on the radical, can account for such an increase in the extent of the magnetic interaction. Unusually high values of χT are reached at low temperature, such as 258 emu K mol^{-1} (μ_{eff} = 45 μ_B) at 5 K, which cannot be justified by the previously mentioned model. This observation suggests a phase transition to a ferromagnetically ordered state. Below 5 K a rapid decrease in the χT product is observed, which corresponds to a plateau in the χ vs T plot.

In Figure 4 we report the molar susceptibility measured at low temperature with a SQUID magnetometer operating at 100 Oe as well as the real, χ', and imaginary χ'', components of the susceptibility measured with an AC susceptometer working at zero applied field and at 333 Hz. χ' shows a maximum at ca. 4.8 K, and at this temperature χ'' becomes different from zero and increases rapidly.

The presence of out of phase susceptibility in zero applied field is a clear indication of the onset of magnetic order. The decrease of χ' below T_c is often observed in these kinds of materials, which have a low magnetic density that determines low demagnetizing fields and large domains. In spite of the low coercitive field observed in these materials close to the critical temperature,[10,11] the displacement of the domain walls to follow the oscillating field is almost completely hampered even at low frequency.[30] The static susceptibility remains however almost constant below T_c at a value that is in good agreement with the value expected for a ferromagnet, $\chi^v = 1/N$,[31] where N is the demagnetizing factor, which agrees well with that calculated on the basis of the geometry of the sample.[32] The present critical temperature is the lowest observed to date in Mn–NITR chain compounds. In fact T_c = 7.6 K for R = isopropyl,[10] while for ethyl and n-propyl it is 8.1 and 8.6 K, respectively.[11]

(24) Verdaguer, M.; Gleizes, A.; Renard, J. P.; Seiden, J. *Phys. Rev. B* **1984**, *29*, 5144.
(25) Pei, Y.; Kahn, O.; Sletten, J. *J. Am. Chem. Soc.* **1986**, *108*, 3143.
(26) Coronado, E.; Drillon, M.; Nugteren, P. R.; de Jongh, L. J.; Beltran, D. *J. Am. Chem. Soc.* **1988**, *110*, 3907.
(27) Caneschi, A.; Gatteschi, D.; Renard, J. P.; Rey, P.; Sessoli, R. *Inorg. Chem.* **1989**, *28*, 2940.
(28) Seiden, J. *J. Phys. Lett. (Paris)* **1983**, *44*, L947.
(29) The agreement factor $r = (\sum(\chi T_{calc} - \chi T_{obs})^2/\sum(\chi T_{obs})^2)^{1/2}$ is 1.3 × 10^{-3}.
(30) Palacio, F.; Lazaro, F. J.; van Duyneveldt, A. J. *Mol. Cryst. Liq. Cryst.* **1989**, *176*, 289.
(31) χ^v is the magnetic susceptibility per unit of volume (cm^3).
(32) Morrish, A. H. *The Physical Principles of Magnetism*; John Wiley & Sons: New York, 1966.

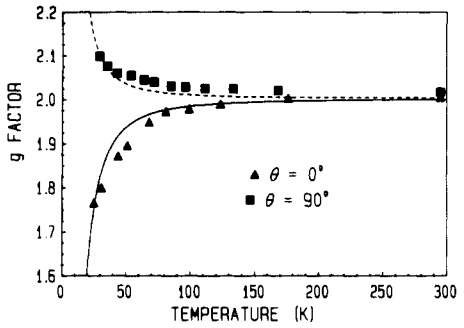

Figure 7. Temperature dependence of the g factor observed in the single-crystal EPR spectra recorded parallel ($\theta = 0°$) and perpendicular ($\theta = 90°$) to the chain direction c. The lines correspond to the calculated values (see text).

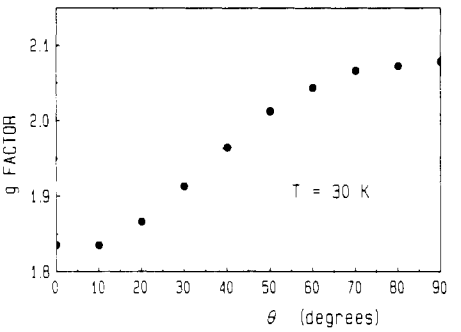

Figure 8. Angular dependence of the g factor at low temperature. θ is angle of the magnetic field with the c axis.

In order to better characterize the nature of the phase transition, magnetization measurements have been performed at 3 K and the results are plotted in Figure 5. The magnetization increases very rapidly, ruling out metamagnetism, and reaches a plateau at about 22000 emu mol^{-1} in good agreement with the value expected for a parallel alignment of the spins of the chains (22340 emu mol^{-1}).[10]

EPR Spectra. Microcrystalline powder EPR spectra at room temperature show a single line centered at $g = 2$ and a much weaker line at $g = 4$. The half-field transition is typical of one-dimensional systems in which the exchange narrowing regime is not completely achieved.[33,34] In Figure 6 we report the line width of EPR signals recorded on a single crystal rotating around the a^* direction. Only one rotation is reported, the spectra being isotropic within error when the field is in the ab plane. The line width at room temperature is larger (500 G) along the c axis and decreases monotonically reaching the minimum, 130 G, when the field is perpendicular to the chain direction. At 30 K the line is broader than at room temperature and shows a very flat minimum at about 60° from c (180 G) with a second maximum (210 G) perpendicular to the chain direction.

The observed angular dependence of the line width does not show the characteristic magic angle behavior of one-dimensional systems.[33,34] This anomaly can be justified by keeping in mind that an important feature of the ideal 1-D model is that the principal direction of the dipolar interaction that broadens the EPR line is parallel to the chain direction. In the present compound the two radicals are in cis position so that the principal directions of the dipolar interactions between radical and manganese are roughly perpendicular to each other and are not aligned along the c axis. The anisotropy of the line width is reproduced by using the complete dipolar second moment in agreement with a nonideal 1-D behavior.[33,34]

At about 20 K the spectra begin to show very unusual structures with a variable number of narrow and asymmetric lines whose position and shape markedly depend on the field orientation, as observed in ferromagnetic resonance.

Another important feature of the single-crystal EPR spectra is the temperature dependence of the resonance field. While at room temperature the g factor is isotropic, on the lowering of temperature g increases when the field is perpendicular to the chain direction and decreases when parallel. The temperature variation of the g factor is reported in Figure 7, while the angular dependence of g at 30 K is shown in Figure 8. Below this temperature it is not easy to determine the g value due to the unusual features of the spectra outlined above.

The g shift with the temperature is well documented in ferro-, antiferro-, and 1-D ferrimagnets.[10,11,35-39] The physical origin of the phenomena can be intuitively understood by keeping in mind that at low temperature the correlation length of the spins along the chain become fairly large and even small anisotropy fields tend to orient the spins in some preferred direction. Internal fields add or subtract to the external one depending on the orientation of the external field, thus determining a variation in the resonance field. Nagata and Tazuke have found that the magnetic susceptibilities and the resonance fields are related by[35]

$$B_x = \sqrt{\chi_y \chi_z / \chi_x} B_x^0$$

where x, y, and z are the principal directions of the susceptibility tensors and B^0 is the resonance field in the absence of short-range order. The other resonance fields are calculated by cyclic permutations. The anisotropic susceptibility can be easily calculated in the approximation of classical spins.[40,41]

The analysis of the g shifts is a very valuable tool in order to characterize the magneto-crystalline anisotropy of this type of materials. In fact it permits one to identify the preferred spin arrangement even if crystals large enough to perform magnetic anisotropy measurements are not available.

In the present compound the easy axis lies in the plane perpendicular to the chain direction as often observed in 1-D ferrimagnets in which the principal source of anisotropy is the intrachain dipolar interaction.[39] Due to the C_3 symmetry of the crystal structure, all the orientations in the ab plane have the same energy and the system has a real xy anisotropy.

The numerical treatment of the g shift of Nagata and Tazuke has recently been extended to the case of alternating spin chains.[9,33] The temperature dependence of the g shift of Mn(hfac)$_2$NITPhOMe has been calculated with the intrachain coupling constant $J = 333$ cm^{-1} and the dipolar parameter $D = 0.0045$ cm^{-1}.[9,33] The results are plotted in Figure 7, and the agreement with the experimental data is satisfactory. The actual value of the coupling constant is slightly different from the value obtained from the analysis of the temperature dependence of the susceptibility because in the expression of the g shifts all the spins are treated as classical spins[42,43] and the quantum nature of $S = {}^1/_2$ is not taken into account.

The magnetic anisotropy observed in the paramagnetic phase, which has a dipolar origin, is probably retained also in the ordered state. In order to confirm this, we calculated the dipolar energy assuming the spin structure of a ferrimagnet with all the spins ${}^5/_2$ up and the spins ${}^1/_2$ down. We calculated the dipolar interaction of a manganese–radical pair with all the other spins contained in a sphere of radius 70 Å, choosing two orientations for the magnetic moments: parallel and perpendicular to the chain direction c. The calculation has been performed by using the point

(33) Richards, P. M. In *Local Properties at Phase Transitions*; Editrice Compositori: Bologna, Italy, 1973.
(34) Gatteschi, D.; Sessoli, R. *Magn. Reson. Rev.* **1990**, *15*, 1.
(35) Nagata, K.; Tazuke, Y. *J. Phys. Soc. Jpn.* **1972**, *32*, 337.
(36) Nagata, K. *J. Phys. Soc. Jpn.* **1976**, *40*, 1209.
(37) Gatteschi, D.; Zanchini, C.; Kahn, O.; Pei, Y. *Chem. Phys. Lett.* **1989**, *160*, 157.
(38) Gatteschi, D.; Guillou, O.; Zanchini, C.; Sessoli, R.; Kahn, O.; Verdaguer, M.; Pei, Y. *Inorg. Chem.* **1989**, *28*, 287.
(39) Caneschi, A.; Gatteschi, D.; Zanchini, C.; Rey, P. *J. Chem. Soc., Faraday Trans.* **1987**, *83*, 3603.
(40) Karasudani, T.; Okamoto, H. *J. Phys. Soc. Jpn.* **1977**, *43*, 1131.
(41) Oshima, K.; Okuda, K.; Date, M. *J. Phys. Soc. Jpn.* **1976**, *41*, 475.
(42) Fisher, M. E. *Am. J. Phys.* **1964**, *32*, 343.
(43) Drillon, M.; Coronado, E.; Beltran, D.; Georges, R. *J. Chem. Phys.* **1983**, *79*, 449.

Table IV. Intrachain Coupling, Dipolar Energies, and Observed and Calculated T_c Values for the Series of $Mn(hfac)_2NITR$ Chains[a]

radical	J, cm^{-1} [b]	E^x_{dip}, K	E^y_{dip}, K	E^z_{dip}, K[c]	T_c^{calc}	T_c^{obs}, K	ref
NITPhOMe (I)	344	−0.063	−0.063	0.126	6.1	4.8	this work
NIT*i*-Pr (II)	330	−0.149	−0.126	0.265	8.8	7.6	10
NITEt (III)	258	−0.155	0.063	0.092	8.1	8.4	11

[a] The transition temperature is calculated with the formula reported in the text. [b] The antiferromagnetic intrachain coupling constant has been obtained by the fitting of the susceptibility with the quantic–classic spin model mentioned in the text. [c] The energies stabilizing the different directions of spin alignment are calculated as described in the text, and z corresponds to the chain direction. y corresponds to the b axis for II, while it is in the Mn–radical plane for III.

dipole approximation and by splitting the unpaired electron of the radical in two magnetic moments located halfway between the oxygen and the nitrogen atoms of the NO groups.[44] The spin structure with the magnetic moment in the *ab* plane is the preferred one, as shown by the calculated dipolar energies with the spins oriented parallel and perpendicular to the chain, respectively: $E^d_\perp = -0.063$ K and $E^d_\parallel = 0.126$ K, in agreement with the anisotropy observed in the EPR spectra.

Comparison with Other $Mn(hfac)_2NITR$ Magnets. In the series of $Mn(hfac)_2NITR$ compounds, where the chains are largely separated from each other, the overall dipolar energy is fairly small and is largely determined by the intrachain interactions between neighboring manganese ions and radicals. However, it is the small interchain components that ultimately allow the onset of 3-D order. The strong antiferromagnetic coupling between metal and radical yields high spin correlation lengths, $\xi(T)$, at low temperature. In other words at sufficiently low temperature the spins are correlated in long segments extending to ca. 50 manganese ions and large effective spins are originated in such a way that the weak dipolar interactions are sufficient to induce 3-D magnetic order at relatively high temperatue. The critical temperatures can be roughly estimated by the relation[45]

$$kT_c = \xi(T_c)|E_{dip}|$$

where E_{dip} is the energy stabilizing the preferred spin orientation determined by dipolar interactions.

In Table IV we report the coupling constants, the dipolar energies, and the calculated and the observed critical temperatures for three $Mn(hfac)_2NITR$ chains. The agreement, as far as the order of magnitudes of T_c is concerned, is surprisingly good, if we consider the crude nature of the model. The relative order between the calculated T_c's for the NITPhOMe derivative (I) and the NIT*i*-Pr one (II) is reproduced, but the calculated T_c of the NITEt compound (III) falls in between the first two, while III actually shows the highest T_c.

Compounds I and II have the same anisotropy, which is of the *xy* type. The energies involved are however much smaller in I where the radicals are cis coordinated, and the directions of the dipolar fields for two adjacent radicals are orthogonal to each other, while they are parallel in the trans-coordinated II. In the case of III the dipolar energies have about the same magnitude as in I because the radicals are cis coordinated, but only one direction of spin alignment is stabilized, thus determining an Ising type anisotropy. The formula given above for estimating T_c takes into account the different type of anisotropy only in the dipolar term; however, the dipolar anisotropy can induce a crossover in the dimensionality of the intrachain interaction. The behavior of III in the paramagnetic region at low temperature deviates from that of the 1-D Heisenberg ferrimagnet toward that of the Ising one. Theory predicts much longer correlation lengths[12] for 1-D Ising systems and hence higher transition temperatures to the ordered state. This effect, which has not been considered in the formula of T_c, can justify the discrepancy with the experimentally observed order of T_c.

Conclusions. $Mn(hfac)_2NITPhOMe$ is a further example of a molecular based ferromagnet whose building blocks are manganese(II) ions and nitronyl nitroxides. Despite the large metal–radical coupling constant, the critical temperature is the lowest so far reported in the series. We feel we have shown how for these compounds magneto-crystalline anisotropy drives the critical temperature and structural magnetic correlations begin to be established in this class of compounds. From $Mn(hfac)_2NITPhOMe$ we have learned that stacking interactions can stabilize a helix structure, and this in turn affects the magnetic properties. In other words, for the manganese–radical chains we are learning to differentiate the contributions of the primary and secondary structure to the magnetic properties.

Finally, we want to stress the extremely high potential interest of $Mn(hfac)_2NITPhOMe$ for magneto–optical investigations. Its helix structure provides natural optical activity and also sizeable NLO second harmonic generation properties. Since at low temperature the compound orders ferromagnetically, it will be interesting to investigate the interplay of all these different properties. This shows how indeed molecular based magnetic materials can provide new exciting fields of investigation with potential for applications.

Acknowledgment. We thank Dr. J. Hulliger and Dr. H. Looser for the preliminary measurements of SHG properties. The financial support of the CNR, the Progetto Finalizzato "Materiali Speciali per Tecnologie Avanzate", and MURST is gratefully acknowledged.

Supplementary Material Available: Tables SI–V, listing crystallographic and experimental parameters, anisotropic thermal factors, calculated coordinates of hydrogen atoms, and bond distances and angles (6 pages); a table of observed and calculated structure factors (17 pages). Ordering information is given on any current masthead page.

(44) Benelli, C.; Caneschi, A.; Gatteschi, D.; Pardi, L.; Rey, P. *Inorg. Chem.* **1989**, *28*, 3230.
(45) Villain, J.; Loveluck, J. M. *J. Phys. Lett. (Paris)* **1977**, *38*, L77.